Entanglement Spectrum in the Fractional Quantum Hall Effect

Andrés Schlief
Universidad de los Andes
Physics Department

May 31, 2013

Fifth School on Mathematical Physics: The Mathematics of Entanglement
Universidad de los Andes, Bogotá.

The Fractional Quantum Hall Effect (FQHE)

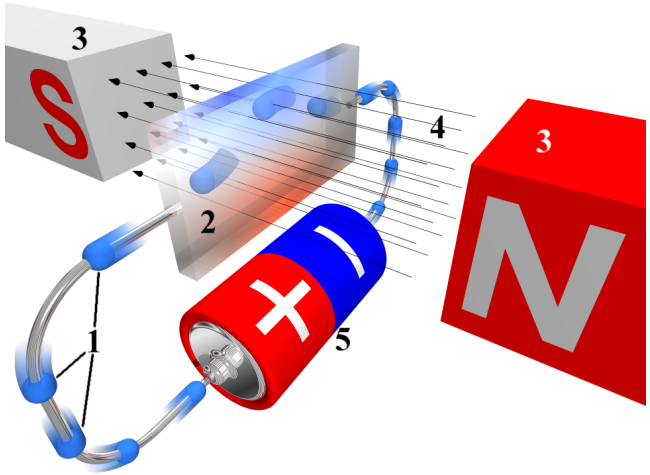

(*a*) The Hall effect [13]

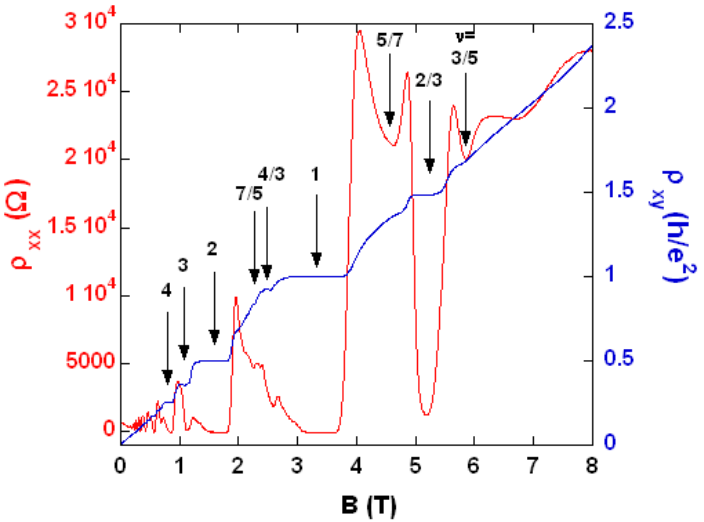

(*b*)Experimental results [12]

First observed in pure low disordered samples of GaAs [10], this is a characteristic phenomenon of interacting electron systems in 2D subject to the following conditions:

- Strong magnetic fields ($|\mathbf{B}| \gg 1$ T).
- Very low temperatures ($T \sim 1$ K).
- Experimentally the *Hall conductivity* is quantized:

$$\rho_{xy}^{-1} = \sigma_H = \nu \frac{e^2}{h}, \ \nu = \frac{N}{N_\phi}$$

- In presence of a uniform magnetic field the electrons occupy Landau levels with the gauge independent energies:

$$E_n = \hbar\omega_c \left(n + \frac{1}{2} \right).$$

- The energy difference between to successive Landau levels scales linearly with $|\mathbf{B}|$, thus, at zero temperature we can focus our attention on the lowest Landau level only ($n = 0$).
- To explain the appearance of the several of the filling factors it suffices to obtain the ground state of the following Hamiltonian:

$$H_N = \sum_{j=1}^{N} \frac{|\boldsymbol{\pi}_j|^2}{2m_e} + \sum_{j<k} v(|\mathbf{r}_j - \mathbf{r}_k|) + \sum_{j=1}^{N} V(|\mathbf{r}|_j) \tag{1}$$

- Them main objective is to focus only in filling factors of the form:

$$\nu = \frac{1}{2m+1}, \qquad m \in \mathbb{N}$$

The Lowest Landau Level (LLL)

- **LLL in $\mathbb{R}^2$:** In the *symmetric gauge* the lowest Landau level is infinitely degenerate and spanned by the following wave functions:

$$\phi_m(\mathbf{r}) = \frac{z^m}{\sqrt{2\pi\ell_B^{2(m+1)} 2^m m!}} \exp\left(-\frac{|z|^2}{4\ell_B^2}\right), \quad m \in \mathbb{N}, \quad z = x + iy, \quad \ell_B^2 = \frac{\hbar}{eB}$$

- In particular these states satisfy the following:

$$\begin{aligned} \pi\langle |z|^2 \rangle_{\phi_m} &= 2\pi\ell_B^2(m+1), \\ L^z \phi_m(\mathbf{r}) &= \hbar m \phi_m(\mathbf{r}). \end{aligned}$$

- **LLL in $\mathbb{T}^2$:** Consider a $L_1 \times L_2$ rectangle with periodic boundary conditions. In the *Landau gauge* the Lowest landau level is finitely degenerate and spanned by the following wave functions:

$$\chi_K(\mathbf{r}) = \frac{1}{\sqrt{\ell_B L_1 \sqrt{\pi}}} \vartheta \begin{bmatrix} \frac{K}{N_\phi} \\ 0 \end{bmatrix} \left(\frac{zN_\phi}{L_1} \middle| \frac{2\pi\ell_B^2 N_\phi^2}{iL_1^2} \right) \exp\left(\frac{(z-\bar{z})^2}{4\ell_B^2} \right),$$

where $K \in \{0, \ldots, N_\phi - 1\}$, $z = x + iy$ and $N_\phi = \frac{L_1 L_2}{2\pi\ell_B^2} \in \mathbb{N}$. This states are located around the directions $y = -\frac{KL_2}{N_\phi}$ and are eigenstates of the magnetic translation operators, which let us interpret K as the eigenvalue of the momentum (generalized) operator.

- **LLL in $\mathbb{S}^2$:** Consider a sphere of radius R and a monopole in the center of the sphere. In the *symmetric gauge*, the lowest Landau level is finitely degenerated and spanned by the following wave functions:

$$\psi_m^S(u,v) = \sqrt{\frac{2S+1}{4\pi}\binom{2S}{m}} u^{2S}\left(\frac{v}{u}\right)^m, \qquad 0 \leq m \leq 2S \in \mathbb{N},$$

where u and v are spinorial coordinates over the sphere. This states satisfy the following relations:

$$\begin{aligned} \langle \cos\theta \rangle_{\psi_m^S} &= \frac{m}{S+1}, \\ L^z \psi_m^S(u,v) &= (S-m)\psi_m^S(u,v). \end{aligned}$$

Laughlin's Ansatz

- **In $\mathbb{R}^2$:** In the infinite plane, the Laughlin wave function is given by [4]:

$$\Psi^{(\kappa)}(\mathbf{r}_1,\ldots,\mathbf{r}_N) = \exp\left(-\frac{1}{4\ell_B^2}\sum_{j=1}^{N}|z_j|^2\right)\prod_{i<j}(z_i-z_j)^{\kappa}, \qquad \kappa=\frac{1}{\nu}.$$

- Since the area of the sample is infinite, here the filling fraction must be interpreted as the following ratio:

$$\nu = \frac{\hbar N(N-1)}{2L^z_{\mathrm{Tot}}}.$$

- This wave function represents a quantum incompressible fluid with uniform density $\sigma_\kappa = (2\pi\kappa\ell_B^2)^{-1}$ which adopts the form of a droplet with effective radius $R=\sqrt{2\kappa N}\ell_B$.

- **In $\mathbb{T}^2$:** In the torus, the Laughlin wave function is given by [5]:

$$\Psi_b^\kappa = \vartheta \begin{bmatrix} \frac{b}{\kappa} + \frac{N_\phi - \kappa}{2\kappa} \\ -\frac{N_\phi - \kappa}{2} \end{bmatrix} \left(\frac{kZ}{L_1} \middle| \kappa \frac{L_2}{L_1} \right) \prod_{j<k} \vartheta_1 \left(\frac{z_j - z_k}{L_1} \middle| \frac{L_2}{L_1} \right)^\kappa \exp\left(\frac{1}{4\ell_B^2} \sum_{j=1}^{N} (z_j - \bar{z_j})^2 \right),$$

where $b \in \{0, \ldots, \kappa - 1\}$, $Z = \sum_j z_j$ and $\vartheta_1(z|\tau)$ is the first Jacobi function. It is worth pointing out that there are κ different wave functions, thus, the ground state of the Hamiltonian is finitely degenerate. In this case the filling fraction adopts its usual form:

$$\kappa^{-1} = \nu = \frac{N}{N_\phi} = \frac{2\pi\ell_B^2 N}{L_1 L_2}$$

- **In $\mathbb{S}^2$:** In the sphere, the Laughlin wave function is given by [2]:

$$\Psi^{\kappa}(\mathbf{r}_1, \ldots, \mathbf{r}_N) = \prod_{j<k} (u_j v_k - u_k v_j)^{\kappa}.$$

- Note that this wave function is essentially the same one on the plane up to some factors. There is a one to one correspondence between Laughlin's ansatz in the infinite plane and Laughlin's ansatz in the sphere, which resembles an stereographic projection.
- The filling fraction in this case takes the usual form:

$$\kappa^{-1} = \nu = \frac{N-1}{2S}$$

Elementary Excitations and Conformal Field Theory (CFT)

- The elementary low energy excitations of Lauhglin's wave function are quasi-holes and quasi-electrons which obey *fractional statistics*. In the plane, quasi-holes can be created adiabatically by piercing the droplet with magnetic flux quanta. This modifies the geometry of a disk shaped droplet to that of a ring. Introduction of a great number quasi-holes in the center of the disk is known as the *conformal limit* where the droplet becomes a thin ring whose width is $\frac{N}{\sqrt{2h\nu}}\ell_B$ where h is the number of quasi-holes [4].
- More important than this excitations are those produced by continuous deformations of the droplet's surface. This deformations must be area preserving and the corresponding excitations are gapless. This type of excitations correspond to the edge states of Laughlin's wave function and they are described by an effective edge theory, namely, the $U(1)$ chiral Conformal Field Theory ($U(1)$ chiral CFT) [1].
- For this edge states the number of states with momentum $k \in \mathbb{N}$ is given by the partition function $p(k)$.

What is 'unique' in the FQHE?

- Two dimensional strongly correlated systems present different properties at zero temperature than almost any other system in condensed matter physics. In particular the FQHE exhibits a new type of order different from the classical or quantum orders that can be described by the paradigm of Landau's symmetry breaking theory.
- This new type of order is *robust upon local perturbations* and cannot be described by a symmetry or a broken symmetry. In particular, this order is characteristic of ground state wave functions and can be characterized by the way the topology of the real space affects these ground states (For example, on a Riemannian surface with genus g, the Laughlin wave function is ν^{-g}-fold degenerate). What is 'unique' in the FQHE is the fact that different trial wave functions (Laughlin, Moor-Read, Pffafian, Composite fermions, etc..) have different orders [11].

This new order has received the name of Topological Order.

- It is worth to point out that this type of order appears in Quantum Dimmer Models, Kitaev's Toric Code and Kitaev's Honeycomb model, within a large set of other strongly correlated 2D systems.

Classical Orders and Topological Orders

- **Classical Orders:** Internal structures associated to classical states of matter that are completely described by Landau's theory of symmetries or Landau's theory of symmetry breaking. They characterize universality classes at finite temperature classical states (Probability distributions).
- **Topological Orders:** Internal structures associated to quantum ground states at zero temperature which cannot be described by Landau's theory of symmetries or Landau's theory of symmetry breaking. Moreover this orders depend strongly on the topology of the space where the physical system takes place [11].

Short range and long range Entanglement

Consider a physical system whose ground state is gapped.

- **Short range Entanglement** The ground state of the system has *short range entanglement* if and only if it can be transformed into a separable state by means of local unitary evolutions.
- **Long range Entanglement** If the ground state of the system cannot be transformed into a separable state by means of local unitary evolutions, ti is said that the state has *long range entanglement*.

According to this definitions, topological order is a pattern of long range entanglement, that is, it characterizes the equivalence classes defined by local unitary evolutions. This is the key that relates entanglement to topological order: By studying the ground state's entanglement properties, its topological order can be characterize [11].

How can we detect topological order?

- Study of the ground state in non trivial manifolds $\Rightarrow$ Often very difficult.
- Topological Entanglement Entropy: For a given bipartition the von Neumman entropy of the reduced density matrix scales as [3, 6]:

$$S(\rho_A) = \alpha L - \gamma + \mathcal{O}(L^{-1}),$$

where $\gamma = \log \mathcal{D}$ is the *topological entanglement entropy*. Here $\mathcal{D}$ is the total quantum dimension (accessible form the underlying Topological Quantum Field Theory (TQFT)). Problem!!

- Entanglement Spectrum Gives more information as it is a set of numbers. The counting structure of 'energy' levels identify directly the CFT and hence, the TQFT. Appearance of an entanglement gap allows to characterize the underlying topological order [7].

Entanglement Spectrum [7]

- Given a pure many particle state $|\Psi\rangle \in \mathcal{H}$, its associated density operator matrix can be written always as:

$$\rho = |\Psi\rangle\langle\Psi| = \exp\left(-H_{\text{Ent}}\right),$$

where H_{Ent} is the *entanglement Hamiltonian*. In this picture the entanglement entropy is equivalent to the thermodynamic entropy of a physical system at temperature $T = k_B^{-1}$ described by a Hamiltonian H_{Ent}.

- The 'energy' spectrum of H_{Enr} is gapped, that is, there is a finite 'energy' gap between the ground state's 'energy' and the 'energy' of the excited states. In particular, when the pure state is separable, this 'energy' gap becomes infinite. This 'energy' gap is known as the *entanglement gap* and the 'energy' spectrum of H_{Ent} is known as the *entanglement spectrum*.
- The entanglement Hamiltonian corresponds to an effective 1D edge Hamiltonian of the corresponding CFT. [8]

- Consider a bipartition of the Hilbert space $\mathcal{H}_A \otimes \mathcal{H}_B$ and the Schmidt decomposition of the pure state $|\Psi\rangle \in \mathcal{H}$:

$$|\Psi\rangle = \sum_i \exp\left(-\frac{\xi_i}{2}\right) |\psi_i\rangle_A \otimes |\phi_i\rangle_B,$$

  where ξ_i are the eigenvalues of H_{Enr} and $\exp(-\xi_i)$ are the eigenvalues of the reduced density matrix $\rho_A = \text{Tr}|\Psi\rangle\langle\Psi|$ subject to the constraint:

$$\sum_i \exp(-\xi_i) = 1.$$

- Observe that if $|\Psi\rangle$ is separable, all the ξ_i are infinite except for one of them whose value is zero. This shows why the entanglement gap is infinite when dealing with separable states.

Signs of Topological Order in the Entanglement Spectrum

- Finite entanglement gap in the thermodynamic limit. This feature is more prominent on *non-abelian* trial wave functions.
- Counting structure in the low lying part of the spectrum. Counting of independent levels in each Virasoro level defines the conformal anomaly $\tilde{c}$ of the CFT and hence, it identifies the underlying TQFT which characterizes the topological order.

For Laughlin states we will focus only in the second feature since Laughlin's wave functions correspond to the FQHE abelian states, where the entanglement gap is not prominent at accessible values of the number of electrons in the system.

Entanglement Spectrum in the FQHE

- In relatively simple geometries the trial wave functions approximating the ground state of the Hamiltonian associated to the FQHE exhibit the system's rotational and translational symmetry. This allows to find well defined quantum numbers that are conserved upon the bipartition of the Hilbert space. In particular, upon the bipartition of the system, the following identities must be satisfied:

$$\begin{aligned} \text{Number of Electrons:} \quad & N_A + N_B = N_{AB}, \\ \text{Angular Momentum:} \quad & L^z_A + L^z_B = L^z_{AB}, \quad \text{(Infinite Plane \& Sphere)} \\ \text{Momentum:} \quad & K_A + K_B = K_{AB}, \quad \text{(Torus)} \end{aligned}$$

Let $\{|\psi_i\rangle\}_{i\in\{1,\ldots,\dim(\mathcal{H}_A)\}}$ an orthonormal base for $\mathcal{H}_A$ and $\{|\phi_i\rangle\}_{i\in\{1,\ldots,\dim(\mathcal{H}_B)\}}$ an orthonormal base for $\mathcal{H}_B$. A general many particle pure state $|\Psi\rangle$ can be written as:

$$|\Psi\rangle = \sum_{i,j} u_{ij}|\psi_i\rangle_A \otimes |\phi_j\rangle_B, \qquad \sum_{i,j}|u_{ij}|^2 = 1$$

It follows that:

$$\begin{aligned}\rho_A &= \mathrm{Tr}_B|\Psi\rangle\langle\Psi| \\ &= \sum_{i,j,m,n,k} u_{ij}u^*_{nm}|\psi_i\rangle_A \otimes \delta_{kj}\langle\psi_n|_A \otimes \delta_{m,k}.\end{aligned}$$

This is, the reduced density matrix will have a nonzero contribution on the terms $|\psi_i\rangle\langle\psi_n|$ if and only if both of them share the same counterpart on subsystem B. This implies that the states $|\psi_i\rangle$ and $|\psi_n\rangle$ must have the same quantum numbers for momentum and electron number. Thus, the reduced density matrix splits into sectors of N_A and $L^z_A(K_A)$.

Bipartitions on the Hilbert Space

There are three main bipartitions that can be made on the Hilbert space:

- Particle Partition (PP): Both subsystems are chosen such that $\mathcal{H}_A$ has N_A electrons and $\mathcal{H}_B$ has N_B electrons.
- Orbital Partition (OP): The most natural way of making a bipartition on this system. Subsystem $\mathcal{H}_A$ is chosen so that it has the first l_A orbitals and $\mathcal{H}_B$ has the rest l_B orbitals. [7]
- Real Space Partition (RSP): Although no the most natural since electrons are not fixed in a position, is the one that offers more information on how topology affects the states. Consists on dividing the manifold into two complementary regions. [9]

OP and RSP in $\mathbb{R}^2$

Since there are infinite magnetic orbitals in the infinite plane, it is more convenient to develop a RSP of the Hilbert space. In order to conserve the gauge symmetry and the rotational symmetry of the system, this partition is chosen as:

$$\begin{aligned} A &= \{(r,\theta), 0 < r < R\}, \\ B &= \{(r,\theta), R < r\}. \end{aligned}$$

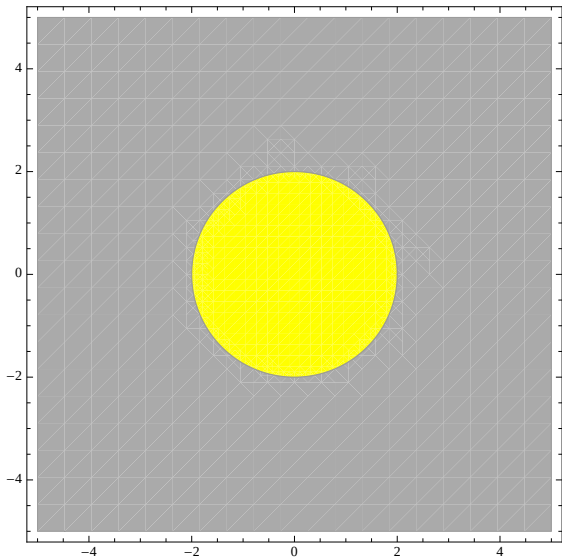

Figure: RSP in $\mathbb{R}^2$

OP and RSP in $\mathbb{T}^2$

For the Torus, in order to conserve the gauge symmetry of the system and its translational invariance, the OP is chosen such that $\mathcal{H}_A$ consists of the first l_A orbitals and $\mathcal{H}_B$ consists of $l_B = N_\phi - l_A$. Note that since states are localized along the lines $y = -\frac{KL_2}{N_\phi}$, an OP resembles a RSP. On the Torus, this OP looks like:

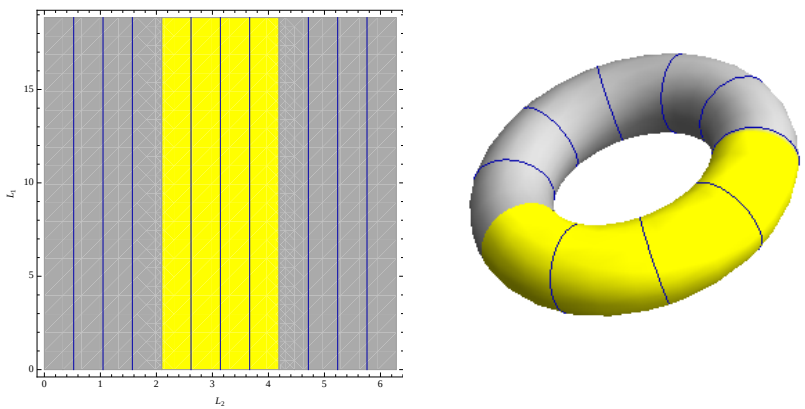

(a) (b)

Figure: OP in $\mathbb{T}^2$. (a) In the finite plane with periodic boundary conditions $L_1 = 2\sqrt{2\pi}\ell_B$ and $L_2 = 6\sqrt{2\pi}\ell_B$. (Blue) Magnetic orbitals locations. (Yellow) Spatial region corresponding to $\mathcal{H}_A$ with $l_A = 4$ orbitals. (Gray) Spatial region corresponding to $\mathcal{H}_B$ with $l_B = N_\phi - l_A = 8$ orbitals. (b) The same as before but viewed in the torus embedded in $\mathbb{R}^3$.

OP and RSP in $\mathbb{S}^2$

The OP on the sphere is similar to the one on the Torus and looking for conservation of gauge an rotational symmetry:

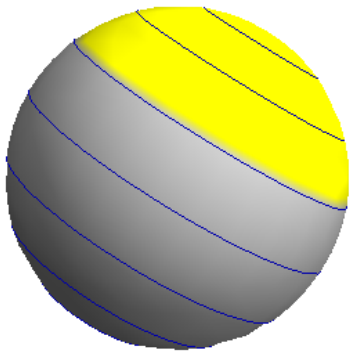

Figure: OP in $\mathbb{S}^2$. (Blue) Localization of the magnetic orbitals for $S = 5/2$. (Yellow) Spatial region corresponding to $\mathcal{H}_A$ choosing $l_A = 3$ orbitals. (Gray) Spatial region corresponding to $\mathcal{H}_B$ with $l_B = N_\phi - l_A = 4$ orbitals.

The RSP is done in such a way that $\mathcal{H}_A$ corresponds to an upper cup of the sphere and $\mathcal{H}_B$ corresponds to its complement. The partition is done with a polar angle $0 < \theta < \Theta$ that divides both regions:

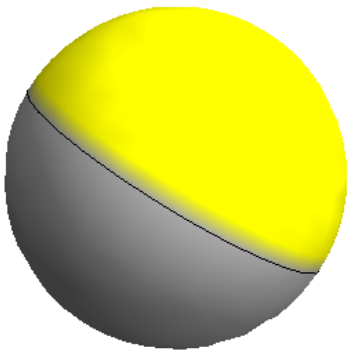

Figure: RSP in $\mathbb{S}^2$.

Numerical Results

- Numerical results for the entanglement spectrum will be presented for OP and RSP. In particular, the OP case will be presented only on the Torus, while the RSP will be presented on the Infinite Plane and the Sphere.
- Let $L^{z,\max}$ and $(K^{\max})$ be the maximum value of the angular (linear) momentum on the entanglement spectrum. Define $\Delta L = L^{z,\max} - L$ $(\Delta K = K^{\max} - K)$ for given values of L (K). Then, the counting structure that the entanglement spectrum shall present corresponds to:

$$\begin{aligned} p(|\Delta L|) &= 1, 1, 2, 3, 5, 7, 11, \ldots, \\ p(|\Delta K|) &= 1, 1, 2, 3, 5, 7, 11, \ldots, \end{aligned}$$

which accounts for the Virasoro counting associated to the $U(1)$ chiral CFT that describes effectively the edge modes of Laughlin's wave function [7, 8].

OES in $\mathbb{T}^2$ for $\nu^{-1} = 3$

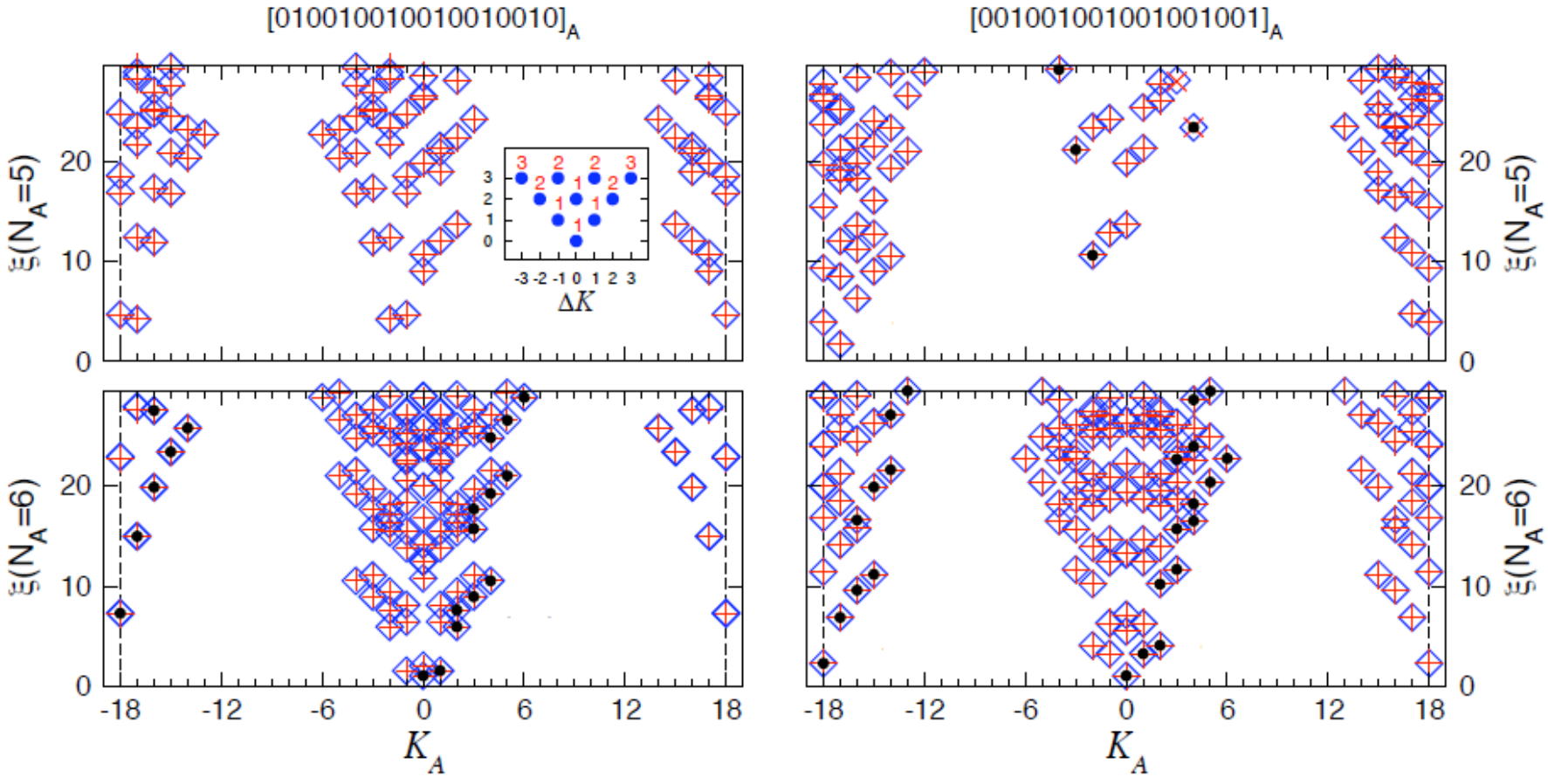

Figure: OP for $N_{AB} = 12$, $N_\phi = 36$ and $L_1 = 10\ell_B$. The partition is such that $l_A = 18$. Inset: Counting structure of the states evidencing the Virasoro counting ($U(1) \times U(1)$ chiral CFT) [5]

RES in $\mathbb{S}^2$ for $\nu = 1$

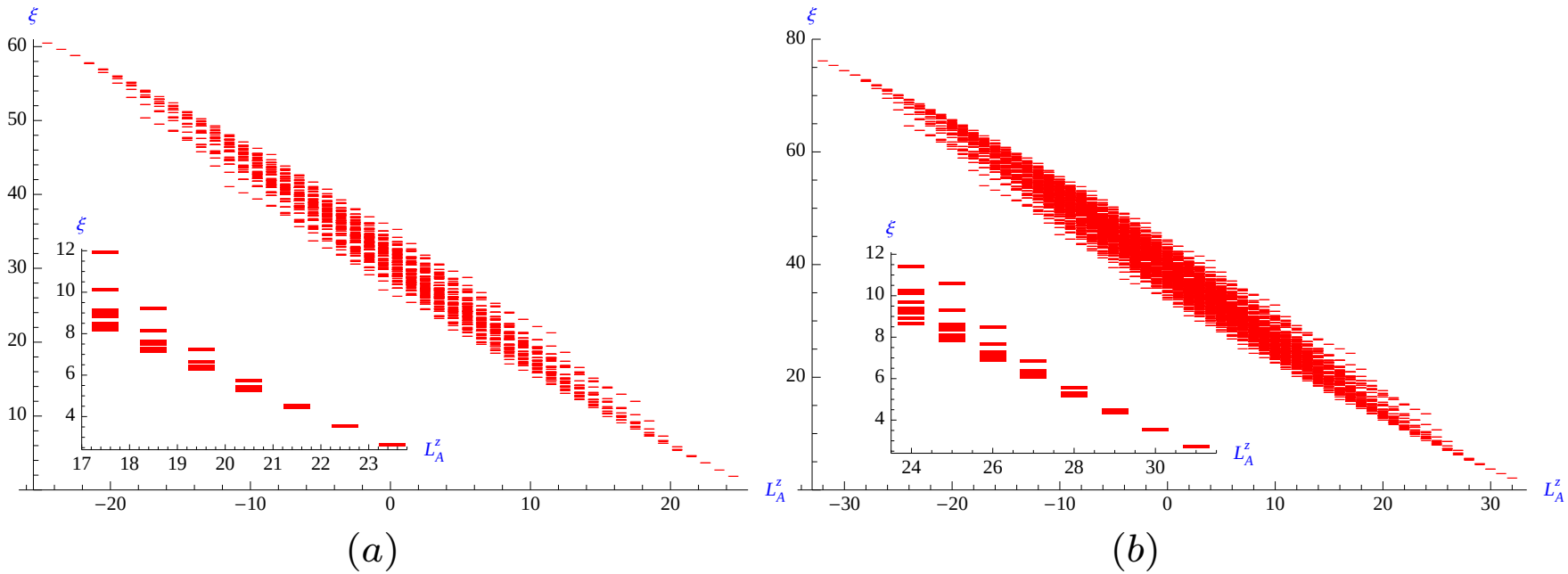

Figure: (a) RES for $N_{AB} = 14$, $N_A = 7$, and choosing the partition at $\Theta = \frac{\pi}{2}$ Inset: Low energy spectrum that evidences the Virasoro counting ($U(1)$ chiral CFT). (b) RES for $N_{AB} = 16$, $N_A = 8$, and choosing the partition at $\Theta = \frac{\pi}{2}$ Inset: Low energy spectrum that evidences the Virasoro counting ($U(1)$ chiral CFT).

RES in $\mathbb{S}^2$ for $\nu^{-1} = 3$

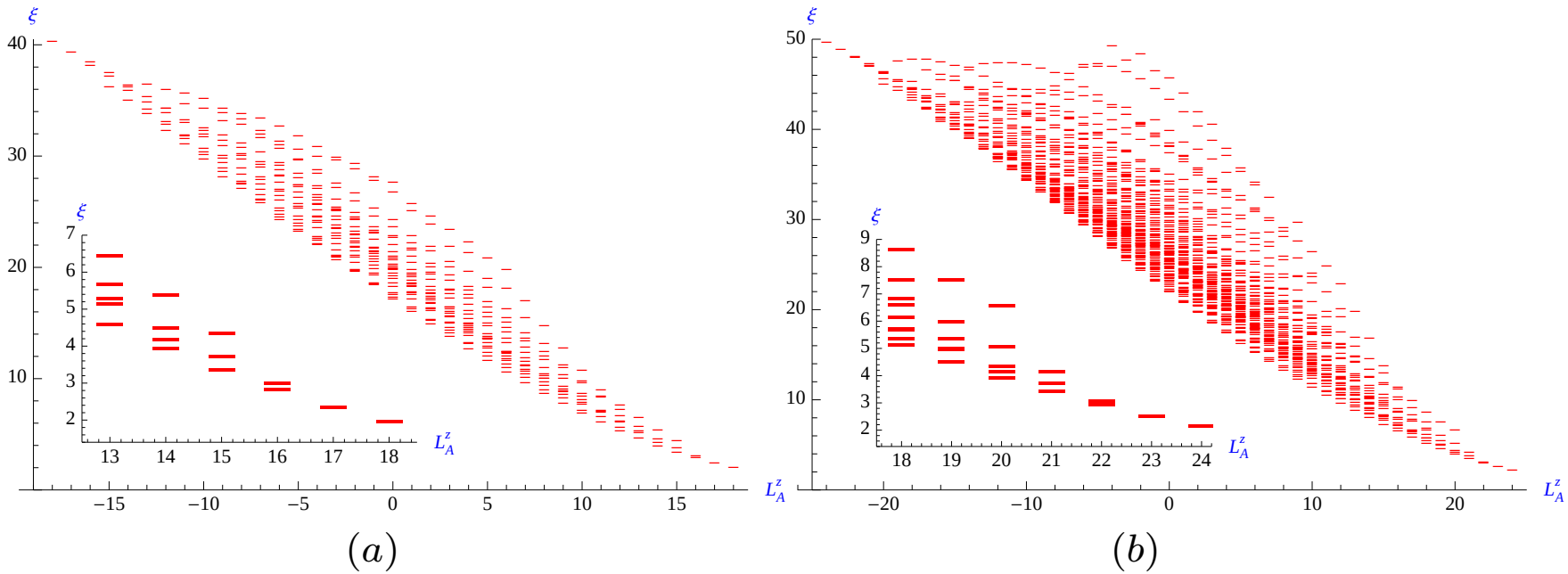

Figure: (a) RES for $N_{AB} = 7$, $N_A = 3$, and choosing the partition at $\Theta \approx \frac{\pi}{2}$ Inset: Low energy spectrum that evidences the Virasoro counting ($U(1)$ chiral CFT). (b) RES for $N_{AB} = 8$, $N_A = 4$, and choosing the partition at $\Theta = \frac{\pi}{2}$ Inset: Low energy spectrum that evidences the Virasoro counting ($U(1)$ chiral CFT).

RES in $\mathbb{S}^2$ for $\nu^{-1} = 5$

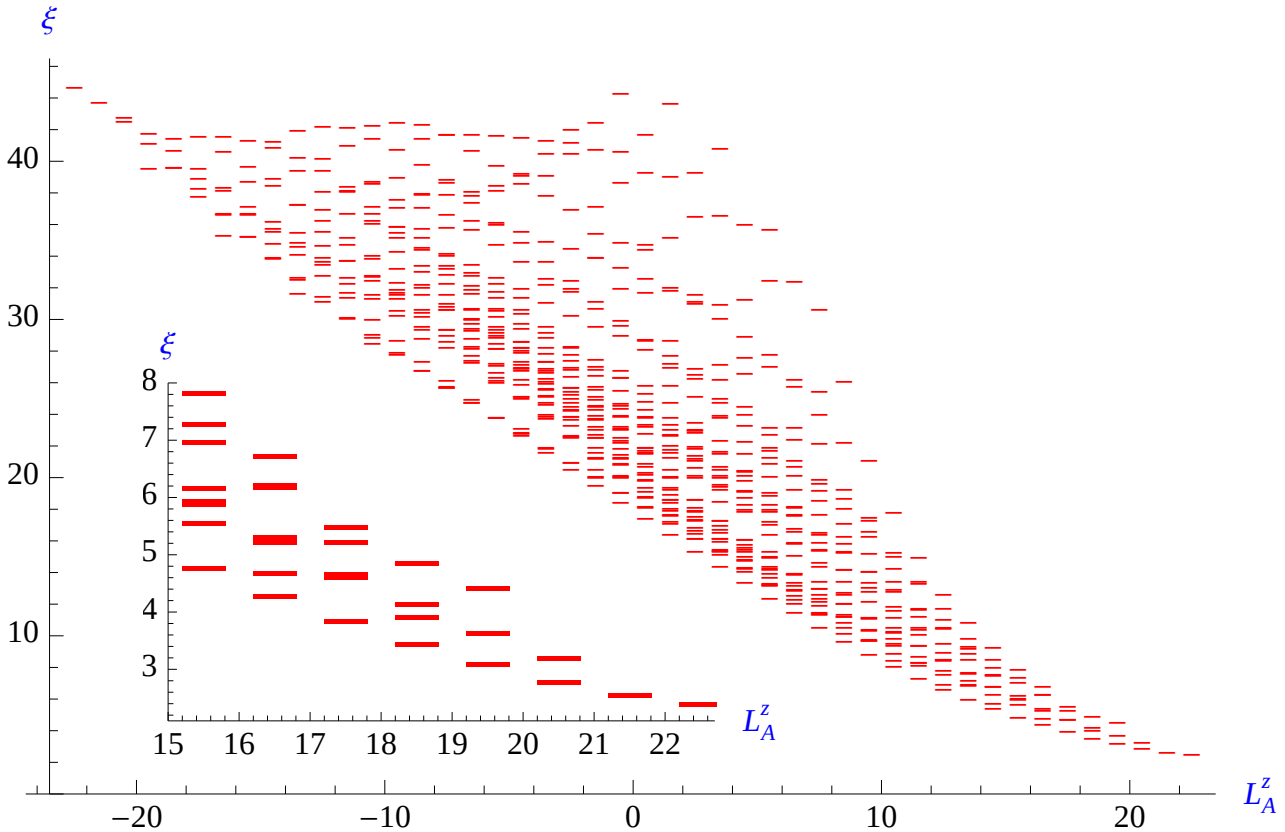

Figure: (a) RES for $N_{AB} = 6$, $N_A = 3$ and $\Theta = \frac{\pi}{2}$. Inset: Lower part of the spectrum showing the Virasoro counting structure ($U(1)$ chiral CFT).

RES in $\mathbb{R}^2$ for $\nu = 1$

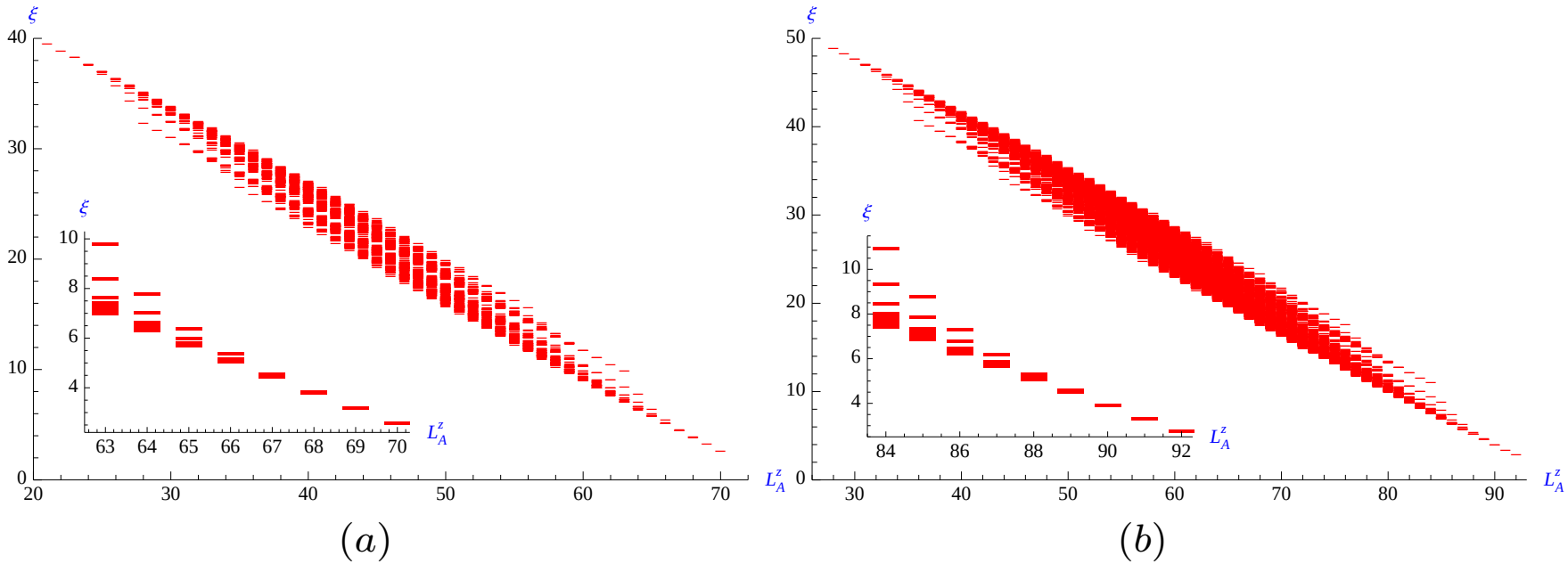

Figure: ((*a*) Real entanglement spectrum of a $\nu = 1$ Laughlin state in the infinite plane with $N_{AB} = 14$ electrons. The partition is such that $N_A = 7$ and $R = \sqrt{13}\ell_B$. Inset: Lower part of the spectrum which evidences the Virasoro counting ($U(1)$ chiral CFT). (*b*) Real entanglement spectrum of a $\nu = 1$ Laughlin state in the infinite plane with $N_{AB} = 16$ electrons. The partition is such that $N_A = 8$ and $R = \sqrt{15}\ell_B$. Inset: Lower part of the spectrum which evidences the Virasoro counting ($U(1)$ chiral CFT).

RES in $\mathbb{R}^2$ for $\nu^{-1} = 3$

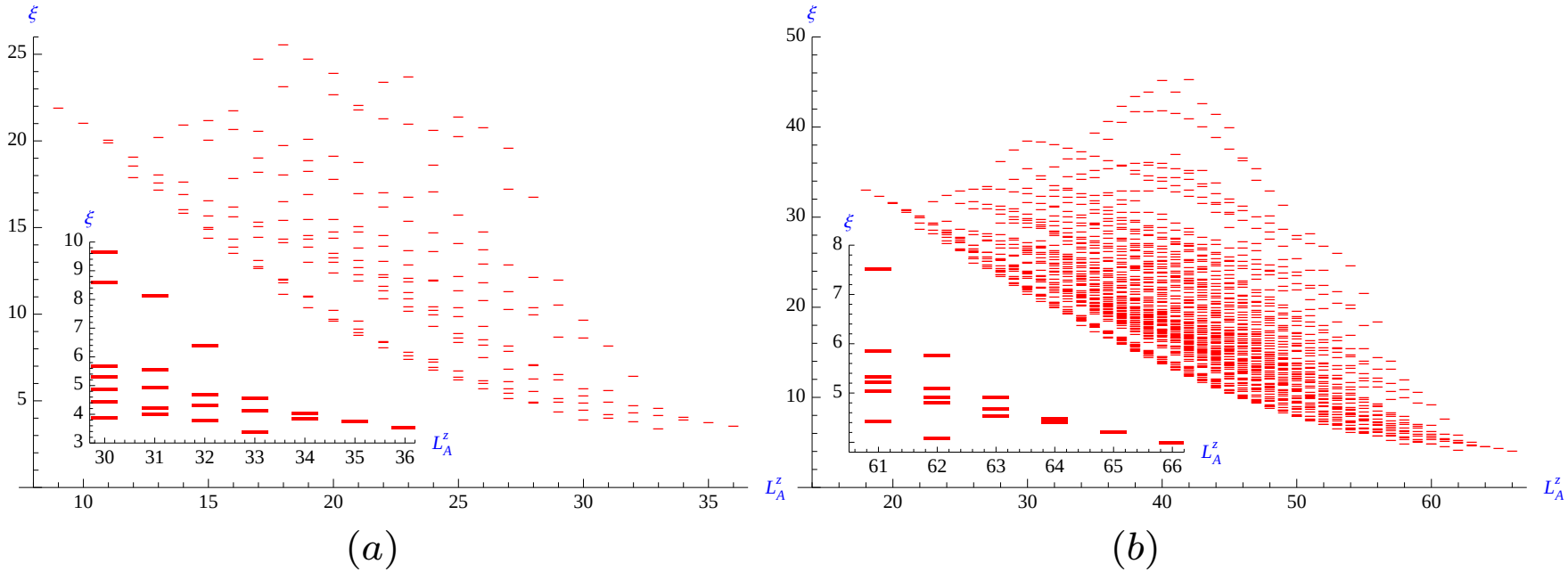

Figure: (a) RES for $N_{AB} = 6$, $N_A = 3$, and choosing the partition at $R = \sqrt{15}\ell_B$ Inset: Low energy spectrum that evidences the Virasoro counting ($U(1)$ chiral CFT). (b) RES with $N_{AB} = 8$ electrons. The partition is such that $N_A = 4$ and $R = \sqrt{21}\ell_B$. Inset: Low lying region of the spectrum which evidences the Virasoro counting ($U(1)$ chiral CFT).

RES in $\mathbb{R}^2$ for $\nu^{-1} = 5$

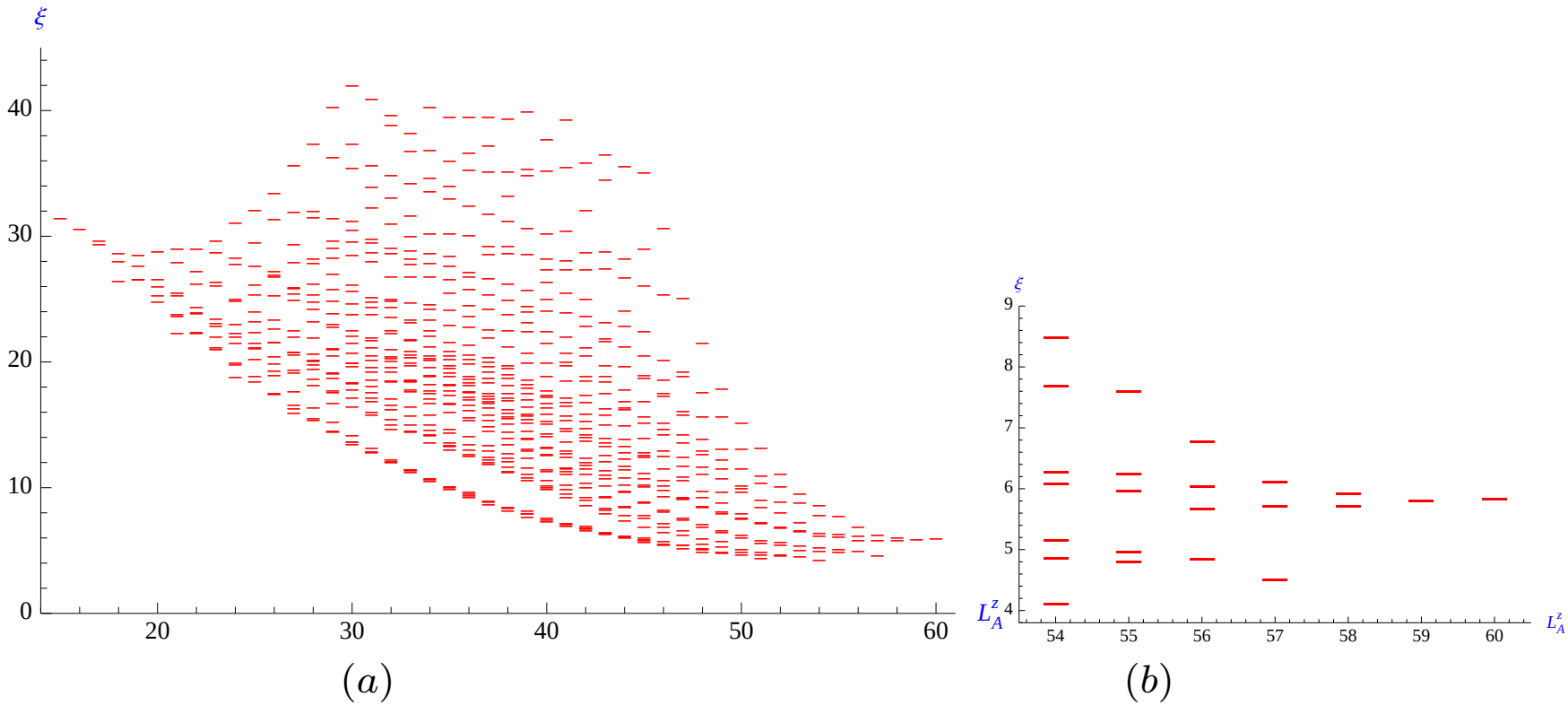

Figure: (a) Real entanglement spectrum of a $\nu = \frac{1}{5}$ Laughlin state in the infinite plane with $N = 6$. The partition is such that $N_A = 3$ y $R = \ell_B$. (b) Low lying region of the spectrum which evidences the Virasoro counting ($U(1)$ chiral CFT)

Introduction of Quasi-holes and the Conformal Limit

$$\Psi^{\kappa,h}(\mathbf{r}_1,\ldots,\mathbf{r}_N)=\prod_{j=1}^{N} z_j^h \Psi^{\kappa}(\mathbf{r}_1\ldots,\mathbf{r}_N)$$

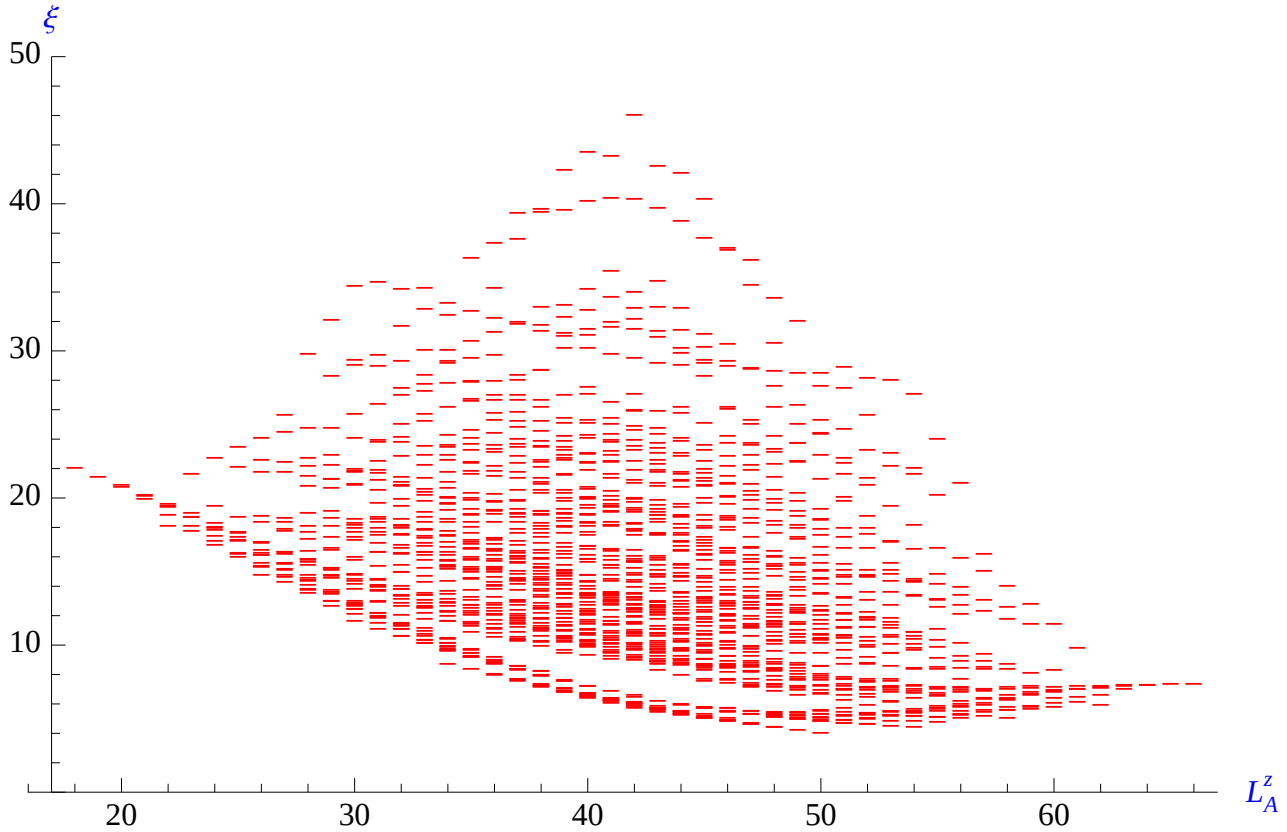

Figure: RES for a $\nu^{-1}=3$ Laughlin state for $N_{AB}=8$ electrons, $N_A=4$ and $R=\sqrt{41}\ell_B$ after adding 20 quasi-holes to the system.

Conformal Limit ($h \to \infty$)

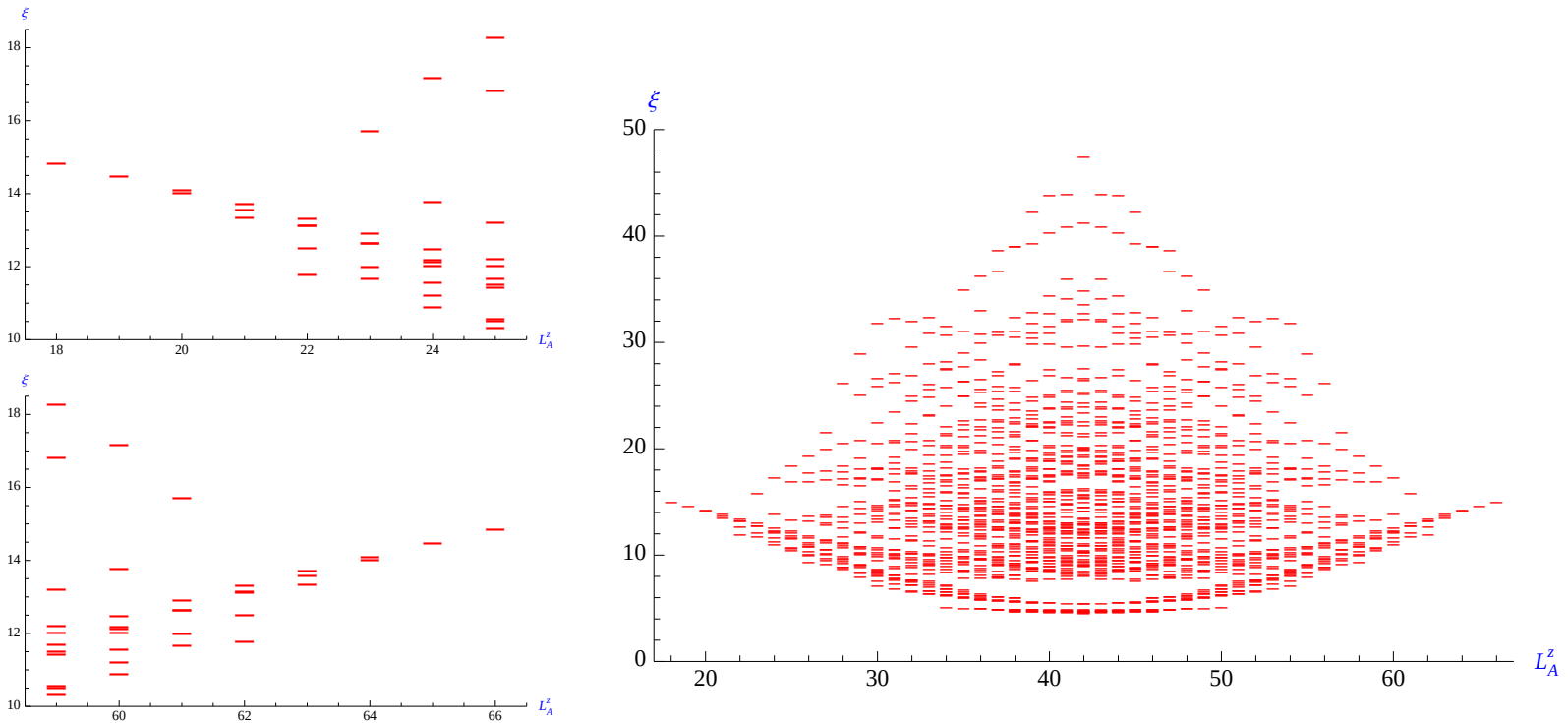

Figure: (Right) RES for the *conformal limit* with $N_{AB} = 8$ y $N_A = 4$. (Up Left) Low part of the spectrum that evidences the mode propagating on the inner ring. (Down Left) Low part of the spectrum that evidences the mode propagating on the outer ring.

Conclusions and Perspectives

- FQHE states, in particular, Laughlin's trial wave function presents a new kind of order: *Topological Order*. In particular this order can be characterized by studying the entanglement properties of the many wave function. In few words, topological order is a pattern of long range entanglement.
- Identification of topological order by means of the Entanglement Spectrum approach allows to extract more information of the ground state wave function than other approaches. However, since the entanglement Hamiltonian corresponds to an effective 1D edge Hamiltonian, this approach is limited (?) to only topological ordered states that present edge states.
- The properties of a topological ordered ground state not only depend on the topology where the physical system is embedded, but depend as well on the topology of the bipartition. ((!)).
- Although the geometries employed have *no boundary*, the study of the system's Entanglement and Entanglement Spectrum provide information on the effective edge theory. That is, the imposition of a bipartition on the system somehow enforces a virtual edge where chiral modes propagate.

- The calculation of the Entanglement Spectrum for the RSP offers more information that that of a OP. In particular, the results presented show that the counting structure characteristic of a $U(1)$ chiral CFT is present in the Entanglement Spectrum up to some point that increases with the size of the system. This determines directly the CFT, its conformal anomaly $\tilde{c}$ and hence, the underlying TQFT that characterizes the topological order.
- Analysis of Laughlin's wave function in the Conformal Limit is a key stone in realizing that the Entanglement Hamiltonian is indeed (up to some normalization constants) the effective Hamiltonian of an effective edge theory.
- General Topological Order Theory: String-net theory and Tensor Category Theory, TQFT, Chern Simons Theories.

[1] A. Capelli, C. A. Trugenberger & G. R. Zemba. arXiv: 9206027v1 (1992).

[2] F. D. M. Haldane, Phys. Rev. Lett **51,** 605 (1983)

[3 A. Kitaev & H. Preskill. arXiv: 0510092v2 (2006).

[4] R. B. Laughlin, Phys. Rev. Lett. **50,** 1395 (1983).

[5] M. Läuchli, E. J. Bergholtz, J. Soursa & M. Haque. arXiv: 0911.5477v2 (2010).

[6] M. Levin & X. G. Wen. arXiv: 0510613v2 (2007).

[7] H. Li & F. D. M. Haldane. Phys. Rev. Lett. **101,** 010504 (2008).

[8] X. L. Qi, H. Katsura & A. W. W. Ludwig. arXiv: 1103.5437v1(2011).

[9] A. Sterdyniak, A. Chandran, N. Regnault, B. A. Bernevi & P. Bonderson. arXiv: 1111.2810v2 (2012).

[10] D. C. Tsui, H. L. Störmer & A. C. Gossard. Phys. Rev. Lett. **48,** 1558 (1982).

[11] X. G. Wen. *An Introduction to Topologicla Orders* Disponible en: `http:// dao.mit.edu/$\sim$wen.`

[12] Image obtained from: `http://www.tasc.infm.it/research/amd/-moddop.php=`

[13] Image obtained from:
http://commons.wikimedia.org/wiki/File:Hall_effect_A.png